Graduate Student Summer Program 2009

Analysis of Errors Associated with the Estimation of Smoke Emission Rates from Satellite Fire Radiative Power Measurements over North America

K. G. THISHAN DHARSHANA

University of Wisconsin-Milwaukee

Department of Mathematical Sciences

(Program in Atmospheric sciences)

Mentor: Dr. Charles Ichoku

NASA Goddard Space Flight Center

Abstract

Fires consume a large amount of biomass in different parts of the world, and emit a substantial amount of smoke to the atmosphere. Fortunately, this smoke emission can be quantified using a recently developed direct linear relationship between the Fire Radiative Power (FRP) measurements from the Moderate Resolution Imaging Spectroradiometer (MODIS) and the Smoke aerosol Emission Rates (SER) derived from MODIS measurements of aerosol optical depth (AOD) and wind fields from the NCEP/NCAR reanalysis data. However, the results are overestimated by about 50%. In an attempt to identify the reasons for this overestimation, scatter plots of SER vs FRP for North America were analyzed together with several environmental variables, and it was revealed that cloud fraction plays a major role. It was found that most of the points that deviated significantly from the linear regression fit were for data corresponding to large cloud fractions. Furthermore, when a particular grid has many ecosystem categories, the corresponding plot does not comply with the expected direct linear relationship, although no single ecosystem type shows any significant influence. The rest of the parameters considered, both static and varying, do not seem to have any influence on the point scatter. It is expected that introducing a way to correct for these error sources would improve the relationship between SER and FRP, and facilitate reliable smoke emission estimates for various important applications such as air quality forecasting and climate models.

Keywords: Fire Radiative Power (FRP), Smoke Emission Rate (SER), ecosystem type, fires

1. Introduction

Vast areas of forest lands, grass lands, and agricultural lands across the globe experience wildfires and other types of biomass-burning, which consume an estimated 5500 - 9200 Tg of biomass annually (Scholes and Andreae, 2000; Chin et al., 2002). Fires release heat energy, which is propagated by conduction, convection, and radiation. Fire Radiative Energy (FRE), like other types of electromagnetic radiant energy, propagates in space and can be remotely sensed with appropriate instruments from aircraft and satellites. Commensurate with the large volumes of biomass consumed by fires annually, tremendous amounts of smoke comprising aerosol particles and trace gases (including CO2, CO, CH4, and other species), are emitted into the atmosphere, where they constitute air pollutants and contribute to the perturbation of the global radiative balance through the scattering and absorption of solar radiation (Ichoku and Kaufman, 2005). Therefore, the effects of fires on living organisms, the environment, and climate are not limited to the ravages of their flame but also include the impacts of the energy, aerosols (or particulate matter-PM), and trace gases emitted into the atmosphere.

Satellite measurements of FRE from MODIS (Moderate-Resolution Imaging Spectroradiometer) which is a sensor aboard two polar-orbiting satellites, Terra and Aqua, launched on December 18, 1999 and May 4, 2002 (Ichoku and Kaufman, 2005) have been used to distinguish fire strengths and to estimate biomass consumption. Since each satellite observation over a given location lasts only an instant, what these sensors actually measure is the rate of release of FRE (R_{fre}) or, simply, the Fire Radiative Power (FRP) in MW (Kaufman et al., 1998; Wooster et al., 2003; Giglio et al., 2006).

With the availability of FRP, attempts have been made to relate FRP with the amount of biomass consumed and/or the amount of smoke aerosols emitted. Results given in Wooster (2002) and Wooster et al. (2005) highlight that there is a linear relationship between the total FRE released over the lifetime of a fire and the total amount of fuel biomass consumed. Apart from that Ichoku & Kaufman (2005) derived another simple linear relationship between FRP and the rate of release of smoke particulate matter for different regions of the world. The latter, which was based on MODIS measurements, was also confirmed in the laboratory using similar measurements of small scale fires (Ichoku et al., 2008b). Consequently, this has enabled the derivation of smoke emission coefficients such that whenever FRP is measured, the corresponding PM emission rate is instantly evaluated. As a result, satellite measured FRP could be used to realistically estimate the smoke emissions as well as the amount of biomass burned both from regional and global scale open-air biomass burning activities (Ichoku et al., 2008a).

However, the above derived linear relationship does not hold perfectly for many of the cases. This could be due to errors in 1) simultaneous observation of fire and emitted smoke; 2) accuracy of MODIS Aerosol Optical Thickness (AOT); 3) conversion of AOT to aerosol mass density; 4) accuracy of NCEP wind fields; 5) smoke plume height assumption; 6) accuracy and consistency of MODIS derived R_{fre}; 7) cloud cover and, 8) heterogeneity of regional/zonal characteristics (Ichoku and Kaufman, 2005). Hence, to utilize this concept in various important applications, such as air quality forecasting and climate studies, it is important to specifically identify the reasons why some of the data do not satisfy this relationship. Thus, the objective of this study is to analyze some of the error sources and identify the factors, which cause some points to scatter away from the linear regression fit between Smoke Emission Rate (SER) and FRP for the North and Central American regions.

2. Methodology

The data sets used for this study were obtained from several different sources, in different formats. Since data for elevation, land water, slope, aspect and ecosystem type over the specified regions were stored in Hierarchical Data Format (HDF), the MATLAB software was used to extract and organize them in a spreadsheet, which is the data format used in this analysis. However, the main data required for computing the Coefficient of Particulate Matter (CePM), including the Terra- and Aqua-MODIS fire and smoke aerosol data, and the NCEP/NCAR meteorological data, were a reformatted version of the data sets used in Ichoku and Kaufman (2005). With Terra crossing the equator approximately at 10:30 AM and 10:30 PM local time, and Aqua at approximately 1:30 AM and 1:30 PM local time, a subset of the MODIS data which is relevant only for daytime passes over the region of interest was used for the current work. The reason for limiting our analysis to daytime data is because fire activity is dominant during the daytime, when it is favored by atmospheric conditions but weakens during the nighttime. To gain a better understanding of the fire diurnal cycle, Figure 1 showcases the distribution of fires in 2002 in our region of interest.

By looking at Figure 1, it is evident that Aqua has more pixels representing locations of fires compared to Terra. This reflects the fact that Terra passes the region in the morning while Aqua passes in the afternoon, during which fire activity tends to be more active due to favorable environmental conditions.

Subsequently, the data were analyzed by grids of 1˚ x 1˚, which is the finest grid resolution used in analyzing regional fire location data in many reports (Westerling et al., 2003). We analyzed only grid boxes with more than 5 days of fires in 2002, and the outcome revealed a significantly small percentage of cases for Terra compared to Aqua, although data from both the satellites were analyzed to ensure full consideration of available information in the region of interest.

As highlighted in Stocks et al. (2003), the energy released during a fire is represented by fire intensity, which in turn can vary significantly both between and within fires depending on fuel type and loading, as well as topographic and meteorological influences. Hence, by choosing the ecosystem type (Table 1 and Figure 2) as a reasonable attribute to consider, the entire region of interest was sub-divided into ten sub-regions (Table 2) in such a way that each region contains a dominant ecosystem type.

Upon categorizing data on each 1˚ x 1˚ grid based on longitude and latitude locations, for each day fires were observed, SER was plotted against FRP. Since it has been proven that SER and FRP has a direct linear relationship, the plots which didn't show an expected y=mx behavior were further analyzed. It's worth emphasizing that many of the plots had large value for correlation coefficient (R) but did not conform to the expected linear pattern. Those grid boxes whose data exhibited such behavior were analyzed further to determine the reasons for such behavior, along with outlier points from strongly fitted y=mx type scatter plots. At the same time, the plots with larger r-values and linear pattern of points were separately analyzed to understand the conditions that enabled good linear fitting. The variables used in the analysis process include both the static parameters such as ecosystem type, elevation, land/water, slope and aspect as well as variables that can change from day to day such as Angstrom exponent, cloud fraction over land, horizontal and vertical wind speeds, temperature, relative humidity, aerosol optical thickness and scan angle.

3. Results and Discussion

Before presenting results of data analysis, having an idea about the distribution of locations with more than 5 days of fire would be beneficial in many ways. Thus, Figure 3 is intended to satisfy this primary understanding.

Having looked at Figure 3, it is clear that many of the fire locations were detected by Aqua satellite compared to Terra; showing that there are probably more fires during the Aqua satellite overpass in the afternoon than during the Terra overpass in the morning.

Moreover, not every region is equally prone to fires. Among the ten sub-regions, which were subjected to analysis in this work, Venezuela, Mexico, US West, US Central and, US East showed significant number of locations with more than 5 days of fire while the rest had only a handful of cases. Therefore, if any region is omitted in the results reported in subsequent sections, it should be understood that it is due to sparseness of data.

While analyzing data, categorizing the grid boxes on the basis of their r-value was initially thought to be an ideal approach. However, as stated in the methodology section, just focusing on the value of r proved to be misleading, because some plots with large r-values showed excessive point scatter. Hence, the r-values were analyzed with their corresponding plots between SER and FRP. For ease of understanding, this could be explained using Figure 4 where only Figure 4 (a) represents the expected relationship between SER and FRP despite large correlation coefficient values in both the cases. Therefore, Figure 4(a) was analyzed to find out the reasons for such a strong correlation while Figure 4 (b) for reasons for such a poor correlation. With this understanding about the process involved in the analysis, the following sections explain the findings based on the parameters used in the analysis process.

3.1 Effect of cloud cover

When the cloud fraction is large (>50%), the point is almost always deviated from the linear regression fit. However, the opposite argument, which is that highly deviated points should coincide with larger cloud fraction, is not necessarily true, as some other factors such as ecosystem type could have influenced the deviation of such points. Moreover, points corresponding to larger value for SER and a reasonably low value for FRP could be easily justifiable with the idea that the satellite sensor wrongly identifies clouds as smoke from fires. On the other hand, when a large FRP value corresponds with a thick smoke, the sensor identifies the central more dense area of the smoke as cloud while only the thin surrounding portion as smoke. Thus, the value of SER becomes smaller despite its actual size.

3.2 Effect of ecosystem type

After analyzing all plots based on two criteria: (i) strong correlation coefficient ($R \geq 0.6$) along with good y=mx fit, and (ii) weak correlation coefficient ($R<0.2$) or points scattering away from the y=mx fit, the results can be summarized in Tables 3 and 4.

Tables 3 reveal that ecosystem type 2 is common both in highly scattered plots as well as strongly correlated plots, especially for Mexican region. This is an indication that type 2 alone does not have any apparent influence on the regression fit between SER and FRP. Based on analyzed data, it is inferred but not yet confirmed, that a single ecosystem type does not have recognizable impact on the deviation of points from the regression fit.

In contrast, when a particular grid box contains many different ecosystem types (after excluding the days and locations with large cloud fraction), in general, it produces a weakly correlated plot (Figure 5). This may mean that a mixture of several ecosystem types in a single grid box assumed homogeneous could be one of the reasons why the points deviate from the expected linear regression fit.

Apart from the above observations, whenever a fire location was assigned to ecosystem type 0 (water), it was manually verified (based on satellite imagery viewed on-line through http://itouchmap.com/latlong.html, accessed on July 15, 2009), and if it actually located on water, it was excluded from the above analysis.

3.3 Effect of other parameters

Despite the fact that analysis process involved the consideration of other parameters such as Angstrom exponent at 470-670 nm wavelength range over land, zonal and meridional wind speeds, vertical wind speed, temperature and relative humidity at 850 mb height, satellite sensor scan angle, maximum and minimum aerosol optical thicknesses at 550 nm channel, none of these parameters showed distinct characteristics between highly scattered plots and strongly correlated plots.

Moreover the calculated total FRP for a particular date in a given grid box is the sum of FRP values of pixels in various locations within that grid. It is important to realize that 1˚ x 1˚ grid is a large area, which could have many different ecosystem types. Therefore, the point representing that grid box on the scatter plot may have been influenced by many different ecosystems at varying levels. That was not accounted in the analysis process. The most concrete conclusions could be derived only when a particular grid box is comprised of only one type of ecosystem.

4. Conclusion

Analysis of plots between SER and FRP for Central and North America revealed that cloud fraction is one of the reasons why some points deviate from the expected linear regression fit. One of the reasons could be that, when the cloud cover is high, the satellite sensor may wrongly identify clouds as smoke, thereby producing a large value for SER. In addition, when a particular grid box has many different ecosystem types, the corresponding plot tends to show points deviated from the expected fit although one ecosystem type did not show any influence on the point scatter. Apart form cloud fraction and ecosystem type, other parameters, both static and variable, do not seem to have a reportable impact on the deviations associated with the plots.

Acknowledgements

This work was done as a requirement for fulfilling my internship responsibilities at NASA Goddard. Although it was only for a short period of time, it helped me in many different ways in strengthening my career. This would not have happened without the kind and appropriate guidance of my mentor, Dr. Charles Ichoku. I would also like to thank Valerie Casasanto for coordinating this program in a smooth way. Finally, I am very grateful for the opportunity to work with the staff at NASA Goddard and to all my friends at GSSP for extending family feeling.

References

Chin, M., P. Ginoux, S. Kinne, O. Torres, B. N. Holben, B. N. Duncan, R. V. Martin, J. A. Logan, A. Higurashi, and T. Nakajima (2002), Tropospheric aerosol optical thickness from the GOCART model and comparisons with satellite and sun photometer measurements, Journal *of Atmospheric Sciences*, *vol. 59*, pp. 461–483.

Giglio, L., I. Csiszar, and C. O. Justice (2006), Global distribution and seasonality of active fires as observed with the Terra and Aqua Moderate Resolution Imaging Spectroradiometer (MODIS) sensors, *Journal of Geophysical Research, 111*, G02016. doi: 10.1029/2005JG000142.

Ichoku, C., and Y. J. Kaufman (2005), A method to derive smoke emission rates from MODIS fire radiative energy measurements, *IEEE transactions on geoscience and remote sensing, Vol 43*, No 11, pp. 2636-2649.

Ichoku, C., L. Giglio, M. J. Wooster, and L. A. Remer (2008a), Global characterization of biomass-burning patterns using satellite measurements of fire radiative energy. *Remote sensing of Environment*, *112*, pp 2950-2962.

Ichoku, C., J. V. Martins, Y. J. Kaufman, M. J. Wooster, P. H. Freeborn, W. M. Hao, S. Baker, C. A. Ryan, and B. L. Nordgren (2008b), Laboratory investigation of fire radiative energy and smoke aerosol emissions, *Journal of Geophysical Research, 113*, D14S09, doi:10.1029/2007JD009659.

Kaufman, Y. J., C. O. Justice, L. P. Flynn, J. D. Kendall, E. M. Prins, L. Giglio, D. E. Ward, W. P. Menzel and A. W. Setzer (1998), Potential global fire monitoring from EOS-MODIS. *Journal of Geophysical Research, 103*, pp 32215−32238.

Scholes, M. and M. O. Andreae (2000), Biogenic and pyrogenic emissions from Africa and their impact on the global atmosphere, *Ambio, vol. 29*, pp 23–29.

Stocks, B. J., J. A. Mason, J. B. Todd, E. M. Bosch, B. M. Wotton, B. D. Amiro, M. D. Flanningan, K. G. Hirsch, K. A. Logan, D. L. Martell, and W. R. Skinner (2003), Large

forest fires in Canada, 1959-1997, *Journal of Geophysical Research-Atmospheres, 108*(D1), 8149, doi:10.1029/2001JD000484.

Westerling, A. L., A. Gershunov, T. J. Brown, D. R. Cayan and M. D. Dettinger (2003), Climate and wildfire in the western United States, *Bulletin of the American Meteorological Society*, *84* (5), 595-604.

Wooster, M. J. (2002), Small-scale experimental testing of fire radiative energy for quantifying mass combusted in natural vegetation fires. *Geophysical Research Letters, 29* (21), 2027. doi:10.1029/2002GL015487.

Wooster, M. J., B. Zhukov, and D. Oertel, (2003), Fire radiative energy for quantitative study of biomass burning: derivation from the BIRD experimental satellite and comparison to MODIS fire products. *Remote Sensing Environment, 86*, pp. 83−107.

Wooster, M. J., G. Roberts, G. L. W. Perry, and Y. J. Kaufman (2005), Retrieval of biomass combustion rates and totals from fire radiative power observations: FRP derivation and calibration relationships between biomass consumption and fire radiative energy release, *Journal of Geophysical Research, 110*, D24311. doi:10.1029/2005JD006318.

Tables

Table 1. IGBP* land cover classification

Ecosystem type	Integer assigned
Water	0
Evergreen needleleaf forest	1
Evergreen broadleaf forest	2
Deciduous needleleaf forest	3
Deciduous broadleaf forest	4
Mixed forests	5
Closed shrubland	6
Open shrublands	7
Woody savannas	8
Savannas	9
Grasslands	10
Permanent wetlands	11
Croplands	12
Urban and built-up	13
Cropland/natural vegetation mosaic	14
Snow and ice	15
Barren or sparsely vegetated	16
Unclassified	-2

* IGBP: International Geosphere-Biosphere Program

Table 2. Regional categorization based on ecosystem type and their territories*

Region	Min_lon	Max_lon	Min_Lat	Max_Lat
Alaska	-170	-140	50	75
Quebec	-80	-55	45	65
Canada West	-140	-120	50	70
Canada Central	-120	-100	50	70
Ontario	-100	-80	50	70
US West	-125	-110	25	50
US Central	-110	-85	25	50
US East	-85	-70	25	45
Mexico	-120	-85	15	25
Venezuela	-80	-45	0	15

* Regions defined in this study are only for the purpose of data analysis and do not conform to actual political boundaries.

Table 3. Ecosystem types for highly scattered plots vs strongly correlated plots in the presence of a dominant ecosystem type (when available) based on Aqua satellite data

Region	Highly scattered	Strongly correlated
Venezuela		2
US Central	12, 10	
US West	1	
Mexico	2, 12	2
US East	4, 13	
Ontario	1	
Alaska		
Quebec		
Canada West	1	
Canada Central	1, 12	

Note: When a particular Reg_ID had many ecosystem categories, it was not included in the above analysis

Table 4. Ecosystem types for highly scattered plots vs strongly correlated plots in the presence of a dominant ecosystem type (when available) based on Terra satellite data

Region	Highly scattered	Strongly correlated
Venezuela		
US Central	12	5
US West	1	
Mexico		
US East		
Ontario		1
Alaska		
Quebec		
Canada West		
Canada Central		

Note: When a particular Reg_ID had many ecosystem categories, it was not included in the above analysis

Figures

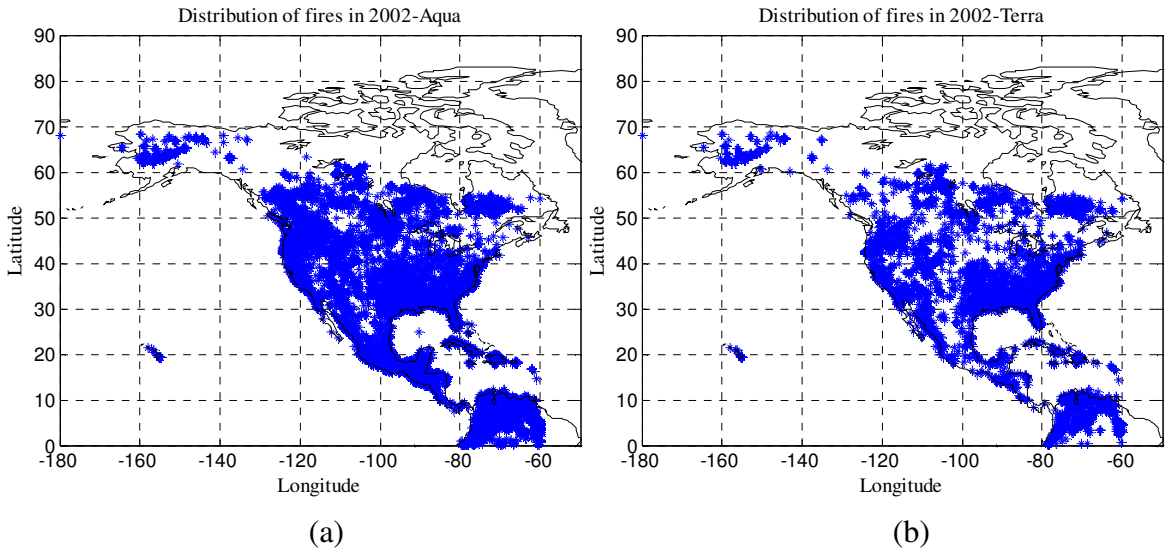

Fig. 1 Distribution of fires in 2002 based on a) Aqua b) Terra satellite data

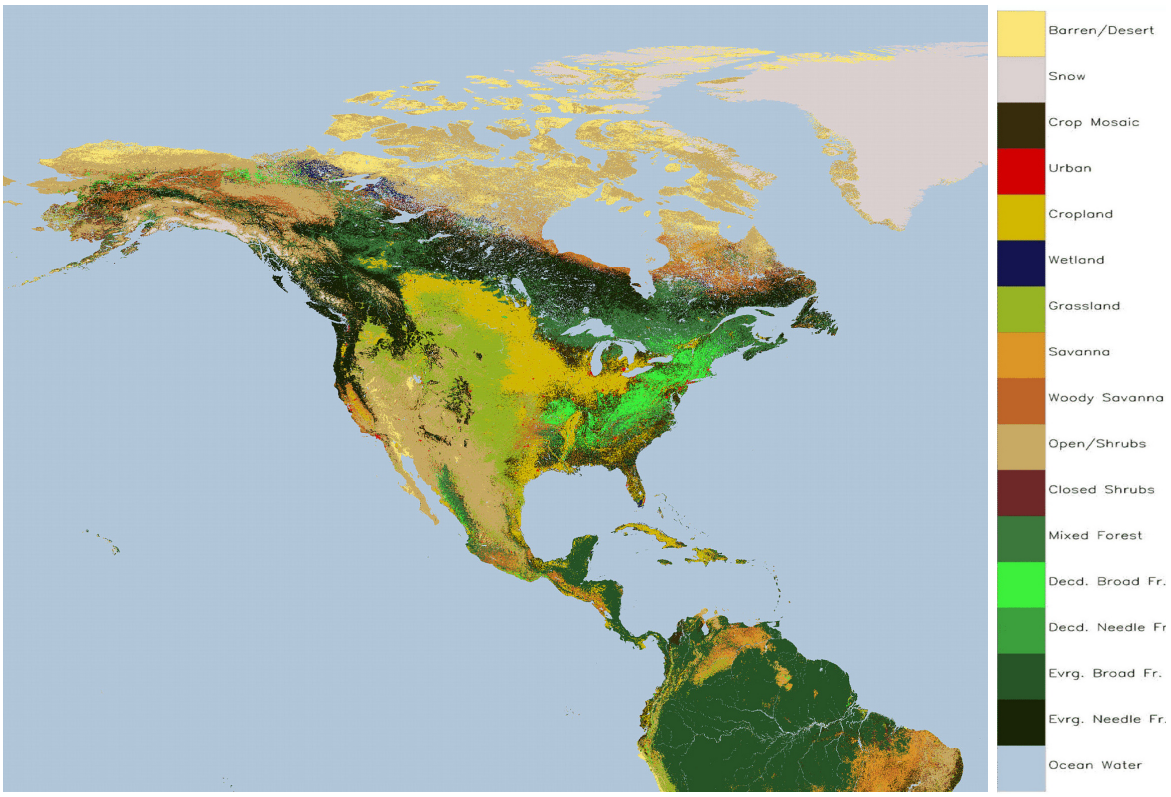

Fig. 2 Land cover map showing some of the main ecosystem types according to the scheme adopted by IGBP.

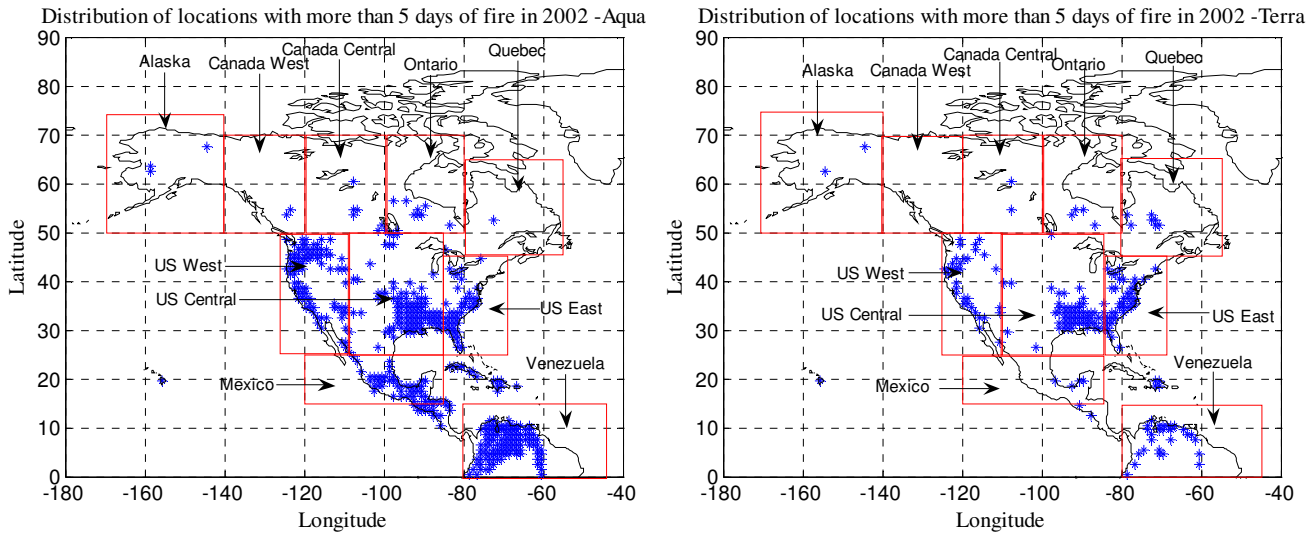

(a) (b)

Fig. 3 Distribution of locations with more than 5 days of fire for a specified grid in 2002 based on a) Aqua b) Terra satellite data

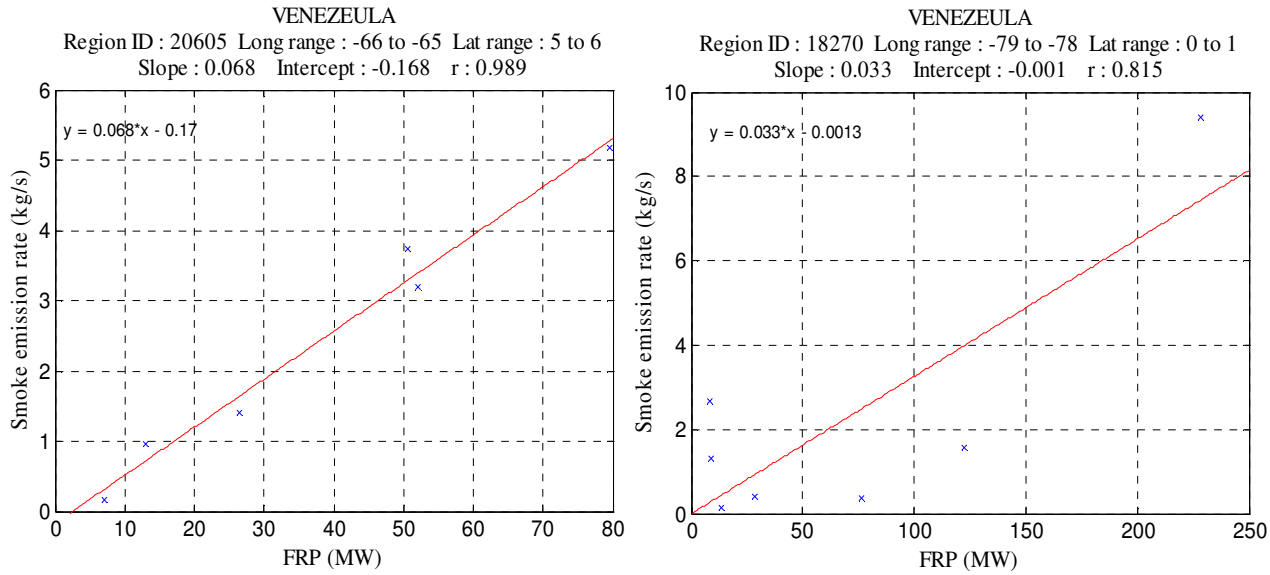

(a) (b)

Fig. 4 Examples that could misdirect the analysis unless looking at the plots: a) desired and b) misleading

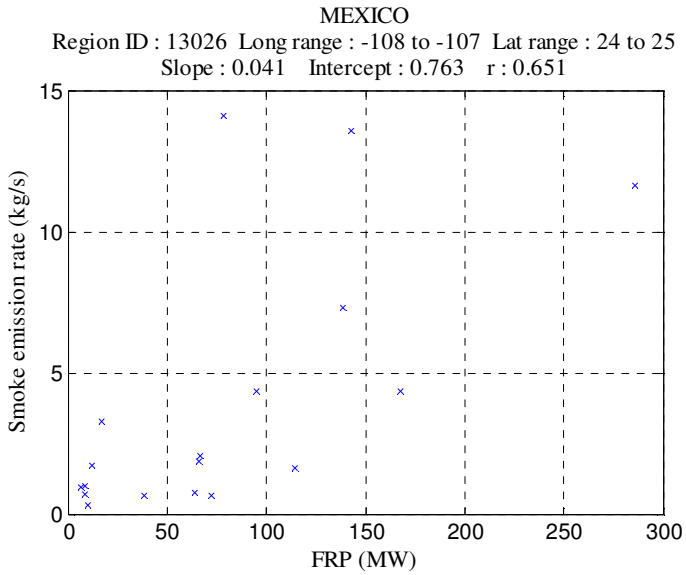

Fig. 5 An example for many different ecosystem types concentrated in one grid.